The Field Perturbation due to a Hollow Cylinder with Radially-Oriented Anisotropic Magnetic Susceptibility: A Model of the Myelin Sheath

Samuel James Wharton[1], and Richard Bowtell[1]

[1]*Sir Peter Mansfield Magnetic Resonance Centre, School of Physics and Astronomy, University of Nottingham, Nottingham, United Kingdom*

Introduction: An understanding of the field perturbations produced by heterogeneous magnetic susceptibility distributions is important in many applications of MRI. In particular, susceptibility-related contrast in phase images of the human brain acquired using gradient echo techniques has been the focus of intense research in recent years [1,2]. This has resulted in the recent demonstration that the magnetic susceptibility of white matter has a measurable anisotropy [2]. The likely source of this anisotropy is the myelin sheath that surrounds axons and specifically, the highly ordered aliphatic chains in the myelin [3]. These long chains are oriented normal to the surface of the myelin layer, such that the magnetic susceptibility in the direction of the local surface normal is expected to differ from that found in the orthogonal directions. Previously, attempts have been made to simulate the field perturbation produced by the myelin sheath using a simple Fourier method which considers only the *z*-component of the induced magnetization [4]. However, recent work by Liu et al. [2] has shown that the *x*- and *y*-components components of the magnetisation must also be considered when calculating field perturbations due to material of anisotropic susceptibility. Here, we derive analytical expressions which characterise the field perturbation due to a model of the myelin sheath consisting of a hollow cylinder in which the magnetic susceptibility is anisotropic and the principal component of the susceptibility tensor is radially directed. The expressions are validated by application of MR-based field mapping to a cylindrical phantom incorporating a pyrolytic graphite sheet (PGS) with a known, highly anisotropic, susceptibility [5].

Theory: Fig. 1 shows a schematic of the model. A long, hollow cylinder with inner radius, r_i, and outer radius, r_o, is placed in a magnetic field, B_0, oriented at an angle, β, to the axis of the cylinder. The cylindrical annulus is populated with material whose susceptibility is characterised by a cylindrically-symmetric susceptibility tensor given by:

$$\underline{\underline{\chi}} = \begin{bmatrix} \chi_{11} & 0 & 0 \\ 0 & \chi_{22} & 0 \\ 0 & 0 & \chi_{22} \end{bmatrix} = \begin{bmatrix} \chi_I & 0 & 0 \\ 0 & \chi_I & 0 \\ 0 & 0 & \chi_I \end{bmatrix} + \begin{bmatrix} \chi_A & 0 & 0 \\ 0 & -\chi_A/2 & 0 \\ 0 & 0 & -\chi_A/2 \end{bmatrix} \quad \text{Eq. 1}$$

where χ_{11} is the susceptibility in the radial direction, while χ_{22} characterises the tangential and longitudinal values (Fig. 1). As shown in Eq. [1], the susceptibility tensor can be split into isotropic, χ_I, and anisotropic, χ_A, parts. The magnetic field perturbation can then be calculated by forming a magnetic scalar potential, and taking its gradient, followed by addition of a sphere of Lorentz correction. The field perturbation for the internal, $r < r_i$, external, $r > r_o$, and annular, $r_o > r > r_i$, compartments is then given by (where r and ϕ are standard cylindrical co-ordinates, see Fig. 1):

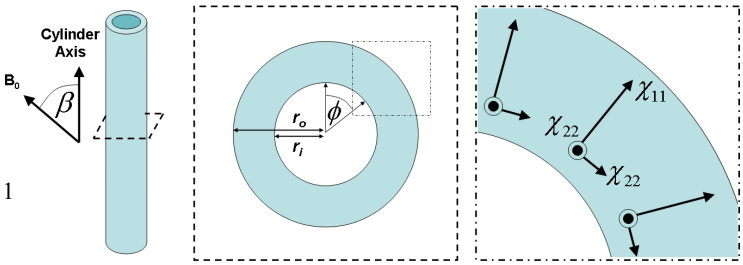

***Fig. 1** Schematic of Hollow cylinder model.*

$$\Delta B(\mathbf{r}) = \begin{cases} \dfrac{B_0 \sin^2\beta\cos 2\phi\left(r_o^2 - r_i^2\right)}{2r^2}\left(\chi_I + \dfrac{\chi_A}{4}\right) & : r > r_o \\ B_0\chi_A\left(\sin^2\beta\left(-\dfrac{5}{12} - \dfrac{\cos 2\phi}{8}\left(1 + \dfrac{r_i^2}{r^2}\right) + \dfrac{3}{4}\log\left(\dfrac{r_o}{r}\right)\right) - \dfrac{\cos^2\beta}{6}\right) & : r_i < r < r_o \\ \quad + B_0\chi_I\left(\dfrac{\cos^2\beta}{2} - \dfrac{1}{6} - \sin^2\beta\cos 2\phi\left(\dfrac{r_i^2}{r^2}\right)\right) & \\ \dfrac{3B_0\chi_A\sin^2\beta}{4}\log\left(\dfrac{r_o}{r_i}\right) & : r < r_i \end{cases} \quad \text{Eq. 2}$$

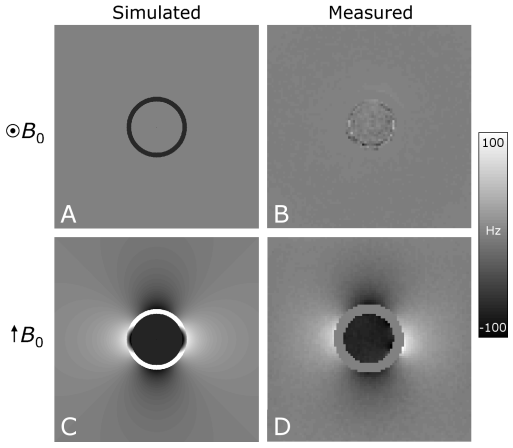

***Fig. 2** Simulated (A&C) and measured (B&D) frequency maps for PGS cylinder parallel (A&B) and perpendicular (C&D) to B_0.*

Methods: To validate the expression in Eq. 2 a pyrolytic graphite sheet (PGS) of 70μm thickness and 55 % purity was wrapped around a 24 mm diameter test tube filled with agar to form a hollow cylinder with χ_I = -114ppm; χ_A = -134ppm [5]. This was placed in a larger test tube inside a 12-cm-diameter, perspex sphere that was filled with agar. The phantom was imaged using a spoiled, 3D gradient echo sequence (FOV = 130x130x50mm^3; resolution = 1 x 1 x 4mm^3; TR = 15ms). The sample was imaged at three echo times (TE = 3, 4, and 5ms) with the long axis of the PGS cylinder first parallel ($\beta = 0^0$) and then perpendicular ($\beta = 90^0$) to B_0. Frequency maps were produced by unwrapping the phase data with respect to TE and then calculating the gradient of the phase evolution, voxel-by-voxel. Subtraction of field maps acquired with and without the PGS, allowed evaluation of the field perturbation produced by the hollow cylinder of anisotropic susceptibility.

Results and Discussion: Measured and simulated frequency maps for the two different orientations are shown in Fig. 2. The measured maps (Fig. 2B&D) agree within error with the simulated data (Fig. 2A&C) in the internal and external compartments. Clearly the frequency offset within the annulus of the PGS, as well as in the small air cavity between the test tube and phantom, could not be assessed, as the proton density was effectively zero in this region. It should be noted that the thickness of the PG annulus has been increased in size in the simulation (with appropriate rescaling of the susceptibility), to allow the field offsets in this region to be visualized. The field perturbation due to a hollow cylinder formed from anisotropic material with a radially-oriented principal susceptibility tensor component is very different from that due to a similar cylinder formed from material of isotropic susceptibility. The most striking difference is found in the internal compartment: for isotropic material the internal frequency offset is zero for all β values, but in contrast, for anisotropic susceptibility a non-zero frequency offset, proportional to $\chi_A\sin^2\beta$, is induced in the internal compartment. The average frequency offset produced in the cylindrical annulus by the anisotropic material is also strongly dependent on β, taking a value of about $-5\chi_A/12$ for a thin annulus (r_0-r_i << r_0, r_i), such that average frequency offsets are of the opposite sign in the sheath and internal cavity (Fig. 2). An important implication of this work is that myelin may induce orientation dependent frequency offsets inside the axonal compartment, which are of opposite sign to those produced inside the sheath. The changes in the relative strengths of the signals from the two compartments with TE resulting from the short T_2^* of myelin water can have a profound impact on phase and magnitude contrast in WM in GE images. The analytic expressions presented here may therefore be valuable for researchers making inferences about WM composition from magnitude or phase images.

References: [1] Duyn et al. PNAS. 2007. (104) 11796-11801; [2] Liu et al. MRM. 2010. (63) 1471-1477; [3] Boroske E. Biophys J. (24) 863-868; [4] Schafer et al. Proc ISMRM. 2011. 4238; [5] Wilson et al. MRM. 2002. (48) 906-914.